Eur. Phys. J. C (2021) 81:926
https://doi.org/10.1140/epjc/s10052-021-09707-3

THE EUROPEAN PHYSICAL JOURNAL C

Regular Article - Theoretical Physics

Dispersion of light traveling through the interstellar space, induced and intrinsic Lorentz invariance violation

I. Brevik[1,a], **M. Chaichian**[2,b], **M. Oksanen**[2,c]

[1] Department of Energy and Process Engineering, Norwegian University of Science and Technology, 7491 Trondheim, Norway
[2] Department of Physics, University of Helsinki, P.O. Box 64, 00014 Helsinki, Finland

Received: 19 August 2021 / Accepted: 1 October 2021 / Published online: 20 October 2021

Abstract Theoretical models and experimental observations suggest that gamma-ray bursts (GRB) and high-energy neutrino bursts travelling through the interstellar space may reach the Earth at different speeds. We propose and study in details the mechanism (i), which always exists, where GRB are slowed down due to the dispersion of light in the interstellar medium. In addition to the standard media such as electrons and photons as CMB, we consider the medium with invisible axions. The amount of GRB delays in different media are calculated in details utilizing a novel technique in QFT by using the hitherto known or estimated densities of particles in the space without introducing any arbitrary parameter. Previously, the GRB delays have been interpreted as a sign of Lorentz invariance violation by modifying the dispersion relation of Special Relativity, which relates the energy, the momentum and the mass of a particle, based on different mechanisms (ii), such as a stringy spacetime foam, coming from a quantum gravity effect and using an adjustable parameter. Obviously, all the above-mentioned mechanisms (i) and (ii) are induced (seeming) Lorentz invariance violations but not an intrinsic (genuine) one. The amount of GRB delay due to the two aforementioned interpretations can be distinguished by observing the time of arrival of light with different frequencies. Namely, dispersion of light (i) predicts that the higher energy GRB arrive the Earth earlier, while in the other interpretations (ii), they arrive later. We notice that the needed amount for delay due to the dispersion of light shall have the potential power to shed additional light on the microstructure of interstellar media with respect to the densities of constituent particles and the origins of their sources. Finally, we indicate the ways to detect the *intrinsic* Lorentz invariance violation and to interpret them theoretically.

[a] e-mail: iver.h.brevik@ntnu.no
[b] e-mail: masud.chaichian@helsinki.fi (corresponding author)
[c] e-mail: markku.oksanen@helsinki.fi

1 Introduction

The propagation of gamma-ray bursts (GRB) in the interstellar medium is a topic that has attracted considerable interest. GRB are highly energetic and diverse events, which are thought to be produced by violent stellar processes, in particular the supernovas and mergers of binary neutron stars. Those events may also produce high-energy cosmic rays and consequently bursts of high-energy neutrinos [1,2]. However, coincident GRB and neutrino bursts have not been observed. The possibility that the neutrino burst could be shifted in time with respect to the GRB is under active study. The time window $\tau = t_{GRB} - t_\nu$ between the arrival times of a GRB, t_{GRB}, and a neutrino burst, t_ν, could vary between seconds or several days. References about this can be found in the report [3] in connection with the ANTARES neutrino telescope. Experimental data taken between 2007 and 2012 were analyzed; gamma-ray energies analyzed were up to 100 TeV. Assuming that a GRB and the corresponding neutrino burst are produced at the same time, a significant delay τ would indicate that the electromagnetic and neutrino signals have travelled at different speeds. Note, however, that the recent experimental studies show only faint neutrino signals associated with GRB [3,4], and hence the observed delays may be inaccurate.

Theoretical interpretations of the GRB delay phenomena have proved to be challenging. Violation of Lorentz invariance at very high energies in the form of modifying the dispersion relation has been considered as a potential interpretation of the delay of high-energy GRB [5–8]. This approach is motivated by various approaches to quantum gravity, as quantum-gravitational fluctuations may lead to a nontrivial refractive index [9]. The stringy spacetime foam is a realization of such an effect [10]. Those are examples of induced violation of Lorentz invariance.

We consider a mechanism within the standard physics. Namely, in the presence of media which interact with pho-

tons, the dispersion of light always occurs what induces changes in the speed of light from its value c in the vacuum. Along this line we study the dispersion of light in several interstellar media and assess the produced GRB delay when photons and neutrinos are assumed to be emitted from the same source and simultaneously. Neither an electron–positron plasma nor a photon medium can account for significant GRB delays, taking the observed or the assumed densities of electrons and photons are too low to slowdown the high-energy photons sufficiently. By a plasma here it is meant a medium where the wave-length of the incoming light is much smaller than the free path of the constituent particles of the medium. Therefore, we study the properties of an axionic medium. Axions are pseudoscalar particles that may both provide a solution to the strong CP problem and as well be a candidate for cold dark matter (CDM). They are not electrically charged but can still interact with photons. Axion electrodynamics has been studied actively and it is connected to topological insulators [11–14]. While the original axion model was ruled out by observations, a new version of the axion, which is called the *invisible axion*, is consistent with laboratory experiments and astrophysical observations [15]. Therefore, an axion medium is a plausible cosmic medium that would have an effect on the propagation of light from distant galaxies. We derive the dispersion relation in an axion medium and assess its effect on the GRB delay.

Our approach is based on the quantum field theory and the optical theorem. We derive the value of of the plasma frequency ω_p, i.e., the term contributing to the change in the speed of light. To our knowledge such a derivation and the result has not been given before. Then the corresponding dispersion relation in this medium and the produced GRB delay are derived.Our estimates show that the interaction between GRB and axions is too weak for producing a significant delay between the gamma-ray and neutrino signals.

To make our physical picture clear: we assume that the photons and neutrinos are emitted from the same source at the same time, and calculate the value of τ in all plausible media in the interstellar space and for a few selected values of the incoming GRB frequency. The dispersive effect indicates that the refractive index will be less than unity, corresponding to the phase velocity being superluminal, while the group velocity is subluminal. We neglect the dissipation effect as this is expected to be weak. At the highest photon frequencies where the permittivity is very close to unity, the photon group velocity is slightly lower than c, so that for these frequencies the delay necessarily has to be the least.

Notice that the interaction of neutrinos with any interstellar medium is extremely weak and hence the dispersion of neutrinos is negligible. Secondly, while the neutrinos are massive and oscillating, the effect on the speed of high-energy neutrinos is very small. Consider a GRB with photon energy 1 TeV and neutrinos with the same energy, $E = 1$ TeV. The dispersion relation $E^2 = p^2c^2 + m^2c^4$ gives the speed of the neutrinos as $v_\nu = \frac{dE}{dp} \approx c(1 - d_\nu)$, where $d_\nu = \frac{m^2c^4}{2E^2}$. Averaging over 3 neutrinos, $\langle m^2c^4\rangle = (1/3)(0.1\,\text{eV})^2$, where the masses are estimated with the heaviest neutrino mass. The speed of neutrinos is given by $d_\nu = 1.7 \times 10^{-27}$. Thus the delay compared to a signal travelling at the speed c would be measured in nanoseconds even for signals from furthest galaxies: $\tau = D \times d_\nu/c \lesssim 10^{-9}$ s, using a maximal travelling distance $D = 1.4\times10^{26}$ m (effective distance to farthest galaxies around $z = 10$). That is a negligible time delay compared to the GRB delays searched in experiments. Some theories of neutrino production in GRB actually predict neutrinos with even higher energy of order 10^2–10^7 TeV [1], which means v_ν might be even closer to c. These arguments justify to take $v_\nu = c$ in our estimates.

The time delay generated by dispersion of light in a medium in its form is essentially different from those caused by the induced Lorentz invariance violations due to quantum gravity effects and in particular a spacetime foam: in the latter cases, the speed of light becomes less for higher energy photon and thus the time delays compared with neutrino bursts grows, a distinguishable effect opposite to the effect of light dispersion in all the media. We shall not consider those (induced) Lorentz invariance breakings in detail here, although some remarks will be given in Sect. 4. We mention though that by assuming a spacetime foam as the cosmic medium, it has been found [9,17] that the delay time is longest for the more energetic photons. This points to an important observation: if one considers one single GRB, the dispersive theory predicts the highest frequencies to move faster, while in the Lorentz violation theory these frequencies will move slower. An experimental test of these theories is thus possible.

Finally, we will mention some remarks and remind of some *intrinsic* Lorentz invariance violation effects.

The Minkowski metric is defined with the signature $(\eta_{\mu\nu}) = \text{diag}(+1, -1, -1, -1)$.

2 GBR delay in usual cosmic media

2.1 Dispersion relation and plasma frequency

A plasma can support both longitudinal and transverse waves. We are interested in transverse waves. Dispersion relation for light in a plasma is [18]

$$\omega^2 = c^2\boldsymbol{k}^2 + \omega_p^2, \tag{1}$$

where ω_p is the plasma frequency, which is due to the plasma oscillations called Langmuir waves, derived from the classical Maxwell equations. The angular frequency is also given as $\omega = \boldsymbol{v}(\hat{\boldsymbol{k}}) \cdot \boldsymbol{k} = \frac{c|\boldsymbol{k}|}{n}$, where n is the refraction index

and $\boldsymbol{v} = \frac{c}{n}\hat{\boldsymbol{k}}$ is the phase velocity, where $\hat{\boldsymbol{k}} = \frac{\boldsymbol{k}}{|\boldsymbol{k}|}$. Thus the refraction index is related to the plasma frequency as

$$n^2 = 1 - \frac{\omega_p^2}{\omega^2}. \tag{2}$$

In an isotropic medium, $\omega = \omega(|\boldsymbol{k}|)$ and $\omega_p = \omega_p(|\boldsymbol{k}|)$, group velocity is parallel to phase velocity, $\boldsymbol{v}_g = v_g\hat{\boldsymbol{k}}$, with the magnitude given as

$$v_g = \frac{\partial\omega(|\boldsymbol{k}|)}{\partial|\boldsymbol{k}|} = c\frac{c|\boldsymbol{k}| + \frac{1}{2c}\frac{\partial\omega_p^2}{\partial|\boldsymbol{k}|}}{\sqrt{\omega_p^2 + c^2\boldsymbol{k}^2}}. \tag{3}$$

Since superluminal propagation of energy and information is forbidden, we demand that the plasma frequency $\omega_p(|\boldsymbol{k}|)$ must satisfy the following condition for any $\boldsymbol{k}$,

$$\frac{c|\boldsymbol{k}| + \frac{1}{2c}\frac{\partial\omega_p^2}{\partial|\boldsymbol{k}|}}{\sqrt{\omega_p^2 + c^2\boldsymbol{k}^2}} \leq 1. \tag{4}$$

We should note that a superluminal group velocity does not imply violation of special relativity, since in such a case the signal velocity is not equal to group velocity [21]. We still consider only cases with $v_g \leq 1$ so that the group velocity can be taken as the signal velocity. If the plasma frequency is independent of $\boldsymbol{k}$, which is the case in a usual plasma with charged particles, and the photon momentum is large compared to the plasma frequency, $c^2\boldsymbol{k}^2 \gg \omega_p^2$, we obtain that group velocity is only slightly lower than c,

$$v_g = \frac{\partial\omega(|\boldsymbol{k}|)}{\partial|\boldsymbol{k}|} \cong c\left(1 - \frac{\omega_p^2}{2\omega^2}\right) \equiv c(1-d), \tag{5}$$

where $d \equiv \frac{\omega_p^2}{2\omega^2} \ll 1$.

2.2 Electron–positron plasma

For an electron–positron plasma, the plasma frequency is obtained from classical electrodynamics [18–20] as (in SI units)

$$\omega_p^2 = \frac{Ne^2}{\epsilon_0 m_e}, \tag{6}$$

where N is the number density of electrons, e^2 is the square of the electric charge of the electron, ϵ_0 is the permittivity of vacuum, and the mass of the electron is $m_e = 9.11 \times 10^{-31}$ kg $= 0.511$ MeV$/c^2$. The same result (6) is obtained from quantum field theory, which is shown in Appendix A. The lightest charged particles have the greatest effect on the dispersion of light. The number density of electrons N is left unspecified for now.

From (6) we get the plasma frequency $\omega_p = 56\sqrt{\bar{N}}$ rad/s, where $\bar{N}$ denotes the number density of electrons as a dimensionless quantity measured in SI units: $\bar{N} = \frac{N}{[N]} = N \times \mathrm{m}^3$, where $[N] = \mathrm{m}^{-3}$. The angular frequency for the gamma-ray energy E is $\omega = 1.5 \times \bar{E} \times 10^{27}$ rad/s, where $\bar{E} = \frac{E}{\mathrm{GeV}}$ is gamma-ray energy in GeV units. We obtain the group velocity (5) of the gamma-ray as

$$v_{GRB} = c\left(1 - 0.7 \times 10^{-45} \times \bar{N}/\bar{E}^2\right). \tag{7}$$

Assume now that $D(z)$ is the effective distance travelled by the photons taking into account the expansion of the Universe. It is defined as [3]

$$D(z) = \frac{c}{H_0}\int_0^z \frac{(1+z')dz'}{\sqrt{\Omega_m(1+z')^3 + \Omega_\Lambda}}, \tag{8}$$

where z is the redshift, H_0 the present Hubble parameter, and Ω_m and Ω_Λ are the standard symbols for the relative matter and dark energy densities. (For an alternative to this method, see [22].) In principle, the photon transit time is

$$t = \frac{D(z)}{v_{GRB}}. \tag{9}$$

In order to evaluate this, one ought to include the z-dependence of v_{GRB} due to the varying density of the plasma. However, we shall ignore the z-dependence of N and v_{GRB} for now, since we are only dealing with some estimates. The time delay between two signals travelling at the speeds (5) and c is obtained as

$$\tau = \frac{D \times d}{c(1-d)} \cong \frac{D \times d}{c}. \tag{10}$$

For the electrons (7) we obtain the GRB delay

$$\tau = 0.7 \times 10^{-45} \times \frac{\bar{N}}{\bar{E}^2} \times \frac{D}{c}. \tag{11}$$

As a first estimate, we may consider galaxy filaments, which are the greatest structures in the universe. The size of the largest filaments is measured in gigaparsecs. While we do not know the electron density in the largest known filaments, we can estimate it with the known electron density of closer filaments. Hence we use the electron density of galaxy filaments around $z = 0.1$ [23]: $N_e = (4.7 \pm 0.2) \times 10^{-4} h_{100}^{1/2}$ cm^{-3} $\approx 4 \times 10^2$ m^{-3}. The effective distance is chosen as $D = 3$ Gpc $= 9 \times 10^{25}$ m. The delay produced by electrons for a GRB propagating through such a structure is estimated as

$$\tau = \frac{0.8 \times 10^{-25}\ \mathrm{s}}{\bar{E}^2}, \tag{12}$$

which is negligible for high-energy photons, in particular for GRB photons with $\bar{E} \geq 1$.

We conclude that the dispersive properties of an electron gas are not significant enough to account for measurable GRB time delays. In fact, even the delay of neutrinos caused by the masses of the neutrinos is much longer than the delay due to dispersion of light in the cosmic electron medium.

2.3 Photon medium

Dispersion of light in photon medium also produces a GRB delay that is far too small to explain the observed delay. Light-on-light scattering has been studied in particle accelerator experiments in great detail. While direct observation of light-on-light scattering is difficult to achieve in particle accelerators [24], evidence for it is increasing and it also used for the search of axion particles [25,26]. When dealing with strong fields this process has attracted considerable interest and new types of experiments have been proposed; cf., for instance, Refs. [27,28].

We obtain from light-on-light scattering [29–33] (see Appendix A.3)

$$\omega_p^2 = \text{const.} \times \frac{N_\gamma e^4}{\omega}, \tag{13}$$

where N_γ is the number density of photons and $\omega = \sqrt{s}/2$ in terms of the invariant s. According to the Planck data on the CMB (Cosmic Microwave Background) radiation, which constitute the majority of photons in the Universe, we have the number density of photons $N_\gamma = (4\text{–}5) \times 10^8\ \text{m}^{-3}$. The GRB delay produced by CMB is estimated as

$$\tau_{\text{CMB}} = \frac{4 \times 10^{-41}\ \text{GeV}^3}{s^{3/2}} \times \frac{D}{c} = \frac{4 \times 10^{-23}}{\bar{E}^{3/2}} \times \frac{D}{c}. \tag{14}$$

For GRB originating from the farthest galaxies the delay produced by the interaction with CMB is $\tau_{\text{CMB}} = 2 \times 10^{-5}\ \text{s}/\bar{E}^{3/2}$; e.g. for a gamma-ray energy $E = 100$ GeV the delay is $\tau_{\text{CMB}} = 2 \times 10^{-8}$ s. This is a very short delay but still much longer than the delay produced by electrons (12).

The extra-galactic background light (EBL) is the second, after the CMB, most abundant part of the photon medium in the Universe. With the data as given in [34,35] (see also [36]), we obtain the photon number density $N_{\text{EBL}} = 10^4\ \text{m}^{-3}$, and with a typical EBL photon energy of 1 eV, we obtain the delay $\tau_{\text{EBL}} = 10^{-32}/\bar{E}^{-3/2} \times (D/c)$. Thus, the number of CMB photons is several orders of magnitude larger than the number of EBL photons and the same is with τ_{CMB} compared with τ_{EBL}.

For high-energy light propagating in the Universe, there also appears the electromagnetic cascades due to the electron–positron pair production, what adds an additional contribution to the ordinary electromagnetic background. However, this process goes through a higher order in the electromagnetic coupling constant and its contribution to the delay τ can be neglected.

Thus the dispersion on background photons does not produce a significant GRB delay.

3 Axions and their effect on the propagation of gamma-rays

Since the GRB delay produced by a charged plasma was found to be proportional to the inverse of the particle mass, $\tau \propto m^{-1}$, it becomes natural to look for particles of much lower mass than the electron. As mentioned above, we will consider a model where the dark matter consists of axions. However, since an electrically charged axion is not consistent with experiments and observations, the plasma frequency formula for charged plasma (6) is no longer valid. Nevertheless, with the vivid activity in axion electrodynamics [11–14] with its connection to topological insulators (for experiment, see CERN Axion Solar Telescope), the assumption of an axionic plasma with its coupling to photons seems quite appropriate. The characteristic axion mass for the QCD axion experiments is about $m_a = 10^{-5}\ \text{eV}/c^2$ [15]. However, the axion mass may be much smaller: a satisfactory agreement with constraints has been reported when the axion mass lies in the interval $10^{-18}\ \text{eV} < m_a < 10^{-28}\ \text{eV}$ [16].

The effective coupling between the axion and two photons is given by the interaction Lagrangian [15,37]

$$\mathcal{L}_{a\gamma\gamma} = -\frac{1}{4} g_\gamma \frac{\alpha}{\pi} \frac{1}{f_a} a(x) F^{\mu\nu}(x) \tilde{F}_{\mu\nu}(x), \tag{15}$$

where α is the fine structure constant and

$$g_\gamma = \frac{1}{2}\left(\frac{\mathcal{N}_e}{\mathcal{N}} - \frac{5}{3} - \frac{m_d - m_u}{m_d + m_u}\right). \tag{16}$$

Here $\mathcal{N}$ and $\mathcal{N}_e$ are respectively the color anomaly and electromagnetic anomaly, m_d and m_u are the quark masses, f_a is the axion decay constant, and $a(x)$ is the axion field. The electromagnetic field strength tensor is $F_{\mu\nu} = \partial_\mu A_\nu - \partial_\nu A_\mu$, and its dual $\tilde{F}^{\mu\nu} = \frac{1}{2}\epsilon^{\mu\nu\rho\sigma} F_{\rho\sigma}$. We define the effective coupling constant g as

$$g = g_\gamma \frac{\alpha}{\pi} \frac{1}{f_a}. \tag{17}$$

If the interaction Lagrangian is written in terms of the electric $\boldsymbol{E}$ and the magnetic field $\boldsymbol{B}$, we would have $\mathcal{L}_{a\gamma\gamma} = -g a(x) \boldsymbol{E} \cdot \boldsymbol{B}$. Here we adopt a system of units with Heaviside–Lorentz electromagnetic units and $\hbar = c = 1$.

First we note that the optical properties of axion backgrounds have been explored in [38,39] and references therein by means of classical axion electrodynamics. The issues concerning GRB have not been considered. The group velocity of light in the presence of the axion field and without charged plasma is given as $v_g = 1 + g^2(\partial_\mu a)^2/8k_0^2$ [38]. If the vector $\partial_\mu a$ is timelike, $(\partial_\mu a)^2 > 1$, the group velocity is not the velocity at which information propagates, and in such cases one should instead use true signal velocity [21]. In order to apply the aforementioned formula for v_g to the problem of GRB delay one would need to obtain the value of $(\partial_\mu a)^2$ along the route of GRB, or relate $(\partial_\mu a)^2$ to the density of

axions. We shall not do that here. Instead we use an approach that is based on quantum field theory.

We would like to mention that while the aim of [38] has been to follow the trajectory of the electromagnetic field to obtain the polarisation vector and the possibility of birefrigence effect, which can occur only in a chiral medium, e.g. in an axionic one, our aim has been to find out the group velocity of GRB travelling through different media such as electron–positron, axion and CMB, each separately, and the delay time for each of them. For that purpose we have considered the dispersion of unpolarized light, and the emerging time delays depending on the photon energy, what is the relevant case for the present GRB experiments. The unpolarized case is obtained in the quantum field theoretical derivation of the scattering amplitude by averaging over the initial polarization states and summing over the final polarization states. In this way the effect of the gyration vector cancels out and no birefringence appears. In future, when the experimental facilities and detectors will have the precision of measuring the polarised GRB bursts with different delay times, the analysis performed in [38] will be most useful.

We derive the dispersion equation (1) for unpolarised coming and detected lights in the axionic matter. A quantum field theoretical calculation of the plasma frequency ω_p^2 is given next. The calculation holds for high-energy photons, when the photon energy is much higher than the mass of the axion m_a. A calculation like this has to our knowledge not been given before, neither in classical electrodynamics nor in quantum field theory.

3.1 Derivation of the dispersion relation of light in axion medium

3.1.1 Calculation of the scattering amplitude

We use the technique illustrated in Appendix A. The effective interaction Lagrangian (15) for invisible axion is

$$\mathcal{L}_{a\gamma\gamma} = -\frac{1}{4} g a F_{\mu\nu}\tilde{F}^{\mu\nu} = -\frac{1}{2} g a \epsilon^{\mu\nu\rho\sigma}\partial_\mu A_\nu \partial_\rho A_\sigma . \tag{18}$$

The Feyman rule for the interaction vertex is read from the interaction Lagrangian as $\frac{i}{2} g \epsilon^{\mu\nu\rho\sigma} k_\mu^{(1)} k_\rho^{(2)}$, where $k^{(1)}$ and $k^{(2)}$ are the four-momenta of the two photons and the free indices ν and σ correspond to the first and second photons, respectively.

We consider scattering of photon on axion, $\gamma + a \to \gamma + a$, at tree level. The scattering amplitude $\mathcal{M}$ is a sum of the two diagrams in Fig. 1.

First we consider the s-channel contribution in detail (first diagram in Fig. 1). Ingoing photon and axion have four-momenta k and p, respectively. The resulting virtual photon propagates with momentum $k + p$. Outgoing momenta are primed k' (photon) and p' (axion), and four-momentum is

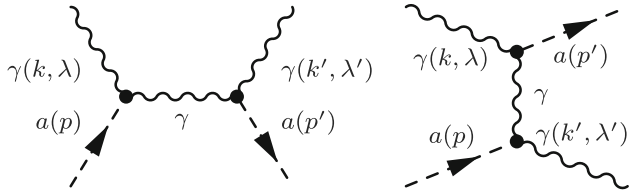

Fig. 1 Feynman diagrams for scattering of photon on axion

conserved $k + p = k' + p'$. The contribution of the s-channel diagram to the scattering amplitude in Feynman gauge is

$$\begin{aligned} i\mathcal{M}_{(s)} &= \frac{i}{2} g \epsilon^{\alpha\beta\gamma\delta}(k_\alpha + p_\alpha)\epsilon_\beta^*(\boldsymbol{k}', \lambda')k'_\gamma \frac{-ig_{\delta\sigma}}{(k+p)^2} \\ &\quad \times \frac{i}{2} g \epsilon^{\mu\nu\rho\sigma} k_\mu \epsilon_\nu(\boldsymbol{k}, \lambda)(k_\rho + p_\rho), \end{aligned} \tag{19}$$

where at the right-hand side of the propagator we have the first vertex. That is simplified as

$$\mathcal{M}_{(s)} = -\frac{3! g^2}{4} \frac{(k_\mu + p_\mu)\epsilon_\nu^*(\boldsymbol{k}', \lambda')k'_\rho k^{[\mu}\epsilon^{\nu}(\boldsymbol{k}, \lambda)p^{\rho]}}{(k+p)^2} \tag{20}$$

using

$$\epsilon^{\mu\nu\rho\sigma} k_\rho k_\sigma = 0 \tag{21}$$

and

$$\begin{aligned} \epsilon^{\alpha\beta\gamma\delta} g_{\delta\sigma} \epsilon^{\mu\nu\rho\sigma} &= -\delta^{\alpha\beta\gamma}_{\mu'\nu'\rho'} g^{\mu'\mu} g^{\nu'\nu} g^{\rho'\rho} \\ &= -3! \delta^{[\alpha}_{\mu'} \delta^{\beta}_{\nu'} \delta^{\gamma]}_{\rho'} g^{\mu'\mu} g^{\nu'\nu} g^{\rho'\rho}. \end{aligned} \tag{22}$$

Then we write out the antisymmetrization of the indices $\mu\nu\rho$ and use the gauge condition $k_\mu \epsilon^\mu(\boldsymbol{k}, \lambda) = 0$,

$$\begin{aligned} \mathcal{M}_{(s)} &= -\frac{3g^2}{2} \frac{1}{(k+p)^2} \big[(k_\mu + p_\mu)k^\mu \\ &\quad \times \epsilon_\nu^*(\boldsymbol{k}', \lambda')\epsilon^\nu(\boldsymbol{k}, \lambda)k'_\rho p^\rho \\ &\quad - (k_\mu + p_\mu)k^\mu \epsilon_\nu^*(\boldsymbol{k}', \lambda')p^\nu k'_\rho \epsilon^\rho(\boldsymbol{k}, \lambda) \\ &\quad - p_\mu \epsilon^\mu(\boldsymbol{k}, \lambda)\epsilon_\nu^*(\boldsymbol{k}', \lambda')k^\nu k'_\rho p^\rho \\ &\quad + (k_\mu + p_\mu)p^\mu \epsilon_\nu^*(\boldsymbol{k}', \lambda')k^\nu k'_\rho \epsilon^\rho(\boldsymbol{k}, \lambda) \\ &\quad + p_\mu \epsilon^\mu(\boldsymbol{k}, \lambda)\epsilon_\nu^*(\boldsymbol{k}', \lambda')p^\nu k'_\rho k^\rho \\ &\quad - (k_\mu + p_\mu)p^\mu \epsilon_\nu^*(\boldsymbol{k}', \lambda')\epsilon^\nu(\boldsymbol{k}, \lambda)k'_\rho k^\rho \big]. \end{aligned} \tag{23}$$

Now use $k^2 = 0$ for the initial photon and $p^2 = m_a^2$ for the axion:

$$\begin{aligned} \mathcal{M}_{(s)} &= -\frac{3g^2}{2} \frac{1}{(2k\cdot p + m_a^2)} \big[\big((k\cdot p)(k'\cdot p) \\ &\quad - (k\cdot p + m_a^2)(k'\cdot k) \big) \epsilon_\mu^*(\boldsymbol{k}', \lambda')\epsilon^\mu(\boldsymbol{k}, \lambda) \\ &\quad + \big((k\cdot p + m_a^2)k^\mu k'_\nu - (k'\cdot p)k^\mu p_\nu \\ &\quad - (k\cdot p)p^\mu k'_\nu + (k'\cdot k)p^\mu p_\nu \big) \\ &\quad \times \epsilon_\mu^*(\boldsymbol{k}', \lambda')\epsilon^\nu(\boldsymbol{k}, \lambda) \big]. \end{aligned} \tag{24}$$

When the momenta of the initial and final photons are parallel (with an angle $\theta = 0$ between $\boldsymbol{k}$ and $\boldsymbol{k}'$), we

have $k \cdot k' = 0$, and we also have $k'_\mu \epsilon^\mu(\boldsymbol{k}, \lambda) = 0$ and $k^\mu \epsilon^*_\mu(\boldsymbol{k}', \lambda') = 0$ from the gauge condition. Thus only the first term of (24) survives in forward scattering. Furthermore, since the momenta of the initial and final photons are parallel, their polarization can be described with same vectors, which are taken to be orthonormal, $\epsilon^*_\mu(\boldsymbol{k}, \lambda')\epsilon^\mu(\boldsymbol{k}, \lambda) = -\delta_{\lambda'\lambda}$. Therefore for $\theta = 0$ the amplitude (24) becomes

$$\mathcal{M}_{(s)}(0) = \frac{3g^2}{2}\delta_{\lambda'\lambda}\frac{(k \cdot p)(k' \cdot p)}{(2k \cdot p + m_a^2)}. \tag{25}$$

Then we assume that axions are very cold so that their linear three-momenta $\boldsymbol{p}$ are very small, $m_a \gg p^i$ and $k_0 \gg p^i$ $(i = 1, 2, 3)$. In the scattering amplitude, we can approximate $k \cdot p = k_0\sqrt{m_a^2 + \boldsymbol{p}^2} - \boldsymbol{k} \cdot \boldsymbol{p} \cong k_0 m_a$. This approximation becomes exact in the rest frame of the initial axion, $\boldsymbol{p} = 0$, which we shall use as the "laboratory frame" of our calculation. Furthermore, we obtain from conservation of four-momentum that $(k + p - k')^2 = p'^2$, where the left-hand side is $2k \cdot p + m_a^2 - 2k'_\mu p^\mu$ in forward scattering and the right-hand side is m_a^2. This implies $k'_0 = k_0$. We obtain

$$\mathcal{M}_{(s)}(0) = \frac{3g^2}{2}\delta_{\lambda'\lambda}\frac{k_0^2 m_a}{(2k_0 + m_a)}. \tag{26}$$

The u-channel contribution (second diagram in Fig. 1) is similar to the s-channel but with the four-momentum of the virtual photon $k + p$ replaced by $k - p'$,

$$\begin{aligned} i\mathcal{M}_{(u)} &= \frac{i}{2}g\epsilon^{\alpha\beta\gamma\delta}(k_\alpha - p'_\alpha)\epsilon^*_\beta(\boldsymbol{k}', \lambda')k'_\gamma \frac{-ig_{\delta\sigma}}{(k - p')^2} \\ &\quad \times \frac{i}{2}g\epsilon^{\mu\nu\rho\sigma}k_\mu \epsilon_\nu(\boldsymbol{k}, \lambda)(k_\rho - p'_\rho). \end{aligned} \tag{27}$$

Thus the u-channel contribution to the forward scattering amplitude is obtained as

$$\mathcal{M}_{(u)}(0) = \frac{3g^2}{2}\delta_{\lambda'\lambda}\frac{(k \cdot p')(k' \cdot p')}{(-2k \cdot p' + m_a^2)}. \tag{28}$$

Using the conservation of four-momentum, we get

$$\mathcal{M}_{(u)}(0) = \frac{3g^2}{2}\delta_{\lambda'\lambda}\frac{k_0^2 m_a}{(-2k_0 + m_a)}. \tag{29}$$

The scattering amplitude for $\theta = 0$ is

$$\begin{aligned} \mathcal{M}(0) &= \mathcal{M}_{(s)}(0) + \mathcal{M}_{(t)}(0) \\ &= \frac{3g^2}{2}\delta_{\lambda'\lambda}\left(\frac{k_0^2 m_a}{(2k_0 + m_a)} + \frac{k_0^2 m_a}{(-2k_0 + m_a)}\right), \end{aligned} \tag{30}$$

and its square for unpolarized photons is

$$\begin{aligned} \frac{1}{2}\sum_{\lambda,\lambda'}|\mathcal{M}(0)|^2 &= \left(\frac{3g^2}{2}\right)^2 \left|\frac{k_0^2 m_a}{(2k_0 + m_a)} + \frac{k_0^2 m_a}{(-2k_0 + m_a)}\right|^2 \\ &= \left(3g^2\right)^2 \left|\frac{k_0^2 m_a^2}{-4k_0^2 + m_a^2}\right|^2. \end{aligned} \tag{31}$$

The amplitude diverges at $k_0 = \frac{1}{2}m_a$, which would generally require regulation. However, here we are concerned with the high-energy case $k_0 \gg m_a$.

The differential cross section for unpolarized photons is

$$d\sigma = \frac{1}{2k_0}\frac{1}{2p_0}\left(\frac{1}{2}\sum_{\lambda,\lambda'}|\mathcal{M}|^2\right) d\text{Lips}, \tag{32}$$

where the relative velocity of the initial particles is $c = 1$ (in any frame) and the Lorentz invariant two-body phase space is the same one as in the case of photon–electron scattering (A.12)–(A.14). The differential cross section is written as

$$d\sigma = \frac{k'_0}{64\pi^2 k_0 p_0 p'_0}\left(\frac{1}{2}\sum_{\lambda,\lambda'}|\mathcal{M}|^2\right) d\Omega. \tag{33}$$

We now choose the rest frame of the initial axion and specialize to forward scattering $\theta = 0$. We have seen that $k'_0 = k_0$ and $p_0 = p'_0 = m_a$, and hence the differential cross section is

$$\begin{aligned} d\sigma(0) &= \frac{1}{64\pi^2 m_a^2}\left(\frac{1}{2}\sum_{\lambda,\lambda'}|\mathcal{M}(0)|^2\right) d\Omega \\ &= \left(\frac{3g^2}{8\pi}\right)^2 \left|\frac{k_0^2 m_a}{-4k_0^2 + m_a^2}\right|^2 d\Omega. \end{aligned} \tag{34}$$

According to (A.8) the absolute value of the forward scattering amplitude is given as

$$|f(0)| = \frac{3g^2}{8\pi}\frac{\omega^2 m_a}{|4\omega^2 - m_a^2|}, \tag{35}$$

where the energy of the photon is given by its angular frequency, $k_0 = \omega$. Unlike in the case of electron–positron plasma, the forward scattering amplitude depends on the photon energy.

Finally, we note that in the dispersion relation (1) we may want to write the plasma frequency as a function of momentum $|\boldsymbol{k}|$ instead of ω. Since the photon of the scattering process is free, we can simply write $\omega = |\boldsymbol{k}|$ in (35),

$$|f(0)| = \frac{3g^2}{8\pi}\frac{\boldsymbol{k}^2 m_a}{|4\boldsymbol{k}^2 - m_a^2|}. \tag{36}$$

3.1.2 Plasma frequency in axion medium

We obtain from (35) that

$$\omega_p^2 = \frac{3Ng^2}{2}\frac{\omega^2 m_a}{|4\omega^2 - m_a^2|}. \tag{37}$$

Recall that our derivation of (A.4) assumed $\omega_p^2 \ll \omega^2$, and hence (37) is valid when

$$\frac{\frac{3}{2}Ng^2 m_a}{|4\omega^2 - m_a^2|} \ll 1. \tag{38}$$

Furthermore, an energy or momentum dependent plasma frequency must satisfy the condition (4). When $\omega > \frac{1}{2}m_a$, the result (37) clearly satisfies the condition (4), since $\frac{\partial\omega_p^2}{\partial|\boldsymbol{k}|} = -3Ng^2\frac{|\boldsymbol{k}|m_a^3}{(4\boldsymbol{k}^2 - m_a^2)^2} < 0$.

Axions are expected to be very light: $m_a \lesssim 10^{-5}$ eV or possibly $m_a \lesssim 10^{-18}$ eV [16]. For photons with energies well above the axion mass, $\omega \gg m_a$, the plasma frequency (37) is nearly constant, i.e. independent of the frequency of the incoming light:

$$\omega_p^2 = \frac{3}{8}Ng^2 m_a\left(1 + \sum_{n=1}^{\infty}\left(\frac{m_a^2}{4\omega^2}\right)^n\right) \cong \frac{3}{8}Ng^2 m_a. \tag{39}$$

If the axion is very light $m_a \lesssim 10^{-18}$ eV, the above result can even be applied to most radio waves. Notice that the result for the dispersion of light in axion medium given in (39) using the Green functions method in quantum field theory, as performed in this work, is new and has not been previously given in the literature.

In the case of gamma-ray bursts, we are deep in the high energy regime. Thus the relevant result is

$$\omega_p^2 = \frac{3}{8}Ng^2 m_a. \tag{40}$$

Note that (40) is proportional to the mean mass density of the axions, $\rho_a = Nm_a$, as

$$\omega_p^2 = \frac{3}{8}g^2\rho_a. \tag{41}$$

Thus only the density of axionic dark matter determines the dispersion of light in the cosmic axion medium.

3.1.3 The delay of gamma-rays in axion medium

The group velocity of gamma-rays in the axion medium is

$$v_{GRB} = 1 - d, \quad d = \frac{3}{16}\frac{g^2\rho_a}{\omega^2}. \tag{42}$$

Estimating the effective coupling constant to be

$$g = 10^{-10}\,\text{GeV}^{-1}, \tag{43}$$

and assuming, according to the GUT models,

$$g_\gamma = \frac{m_u}{m_d + m_u} \approx 0.36, \tag{44}$$

we obtain

$$d = 1.4 \times 10^{-68} \times \frac{\bar{\rho}_a}{\bar{E}^2}, \tag{45}$$

where $\bar{\rho}_a$ is the axion density in units GeV/m^3 and $\bar{E}$ is gamma-ray energy in GeV.

Thus the delay of gamma-rays in the axion medium is

$$\tau = \frac{3}{16}\frac{g^2\rho_a}{\omega^2} \times \frac{D}{c} = 1.4 \times 10^{-68} \times \frac{\bar{\rho}_a}{\bar{E}^2} \times \frac{D}{c}, \tag{46}$$

where D the effective distance traveled by the photons. (As mentioned, we take the velocity of neutrinos to be c.)

As a first estimate, let us consider the Galactic Halo (GH) where dark matter is assumed to consist of axions. The energy density of GH is 0.45 GeV/cm^3 and the radius of GH is 5×10^{20} m [40]. The delay of GRB propagating through the GH is

$$\tau = \frac{1.1 \times 10^{-50}\ \text{s}}{\bar{E}^2}. \tag{47}$$

As a second example, we consider a massive galaxy filament. The average axion density is estimated as $\rho_a = 10^3$ GeV/m^3 and the effective distance is $D = 3$ Gpc $= 9 \times 10^{25}$ m. The delay of GRB is obtained as

$$\tau = \frac{0.7 \times 10^{-48}\ \text{s}}{\bar{E}^2}. \tag{48}$$

The delay is negligible for high-energy photons, as it also is in the case of GH.

We may also comment on the importance of the magnetic field. For an electron–positron plasma, there is no magnetic contribution. By extending to the case of chiral media, the magnetic field comes into play giving an enhancement of g and a reduction of N_a. It is known that for a chiral medium, there is a magnetic contribution to the Casimir effect [41,42].

3.2 Derivation of the dispersion relation of light in photon medium due to axion exchange

When axions exist, photons can interact with each other via axion exchange, in addition to the usual photon-by-photon interaction due to fermion–antifermion loops (box diagrams).

3.2.1 Calculation of the scattering amplitude

We consider scattering of photon on photon $\gamma\gamma \to \gamma\gamma$ at tree level. The scattering amplitude $\mathcal{M}$ is described by the diagrams in Fig. 2.

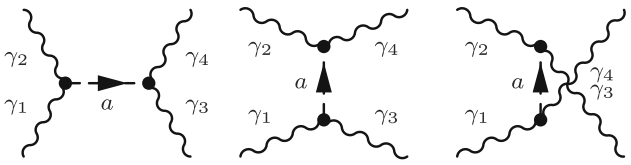

Fig. 2 Feynman diagrams for scattering of photon on photon in axion electrodynamics

The scattering amplitude is written as

$$\begin{aligned} i\mathcal{M} &= \frac{i}{2}g\epsilon^{\alpha\beta\gamma\delta}k_{3\alpha}\epsilon^*_\beta(\boldsymbol{k}_3,\lambda_3)k_{4\gamma}\epsilon^*_\delta(\boldsymbol{k}_4,\lambda_4)\frac{-i}{s-m_a^2} \\ &\times\frac{i}{2}g\epsilon^{\mu\nu\rho\sigma}k_{1\mu}\epsilon_\nu(\boldsymbol{k}_1,\lambda_1)k_{2\rho}\epsilon_\sigma(\boldsymbol{k}_2,\lambda_2) \\ &+\frac{i}{2}g\epsilon^{\alpha\beta\gamma\delta}k_{2\alpha}\epsilon_\beta(\boldsymbol{k}_2,\lambda_2)k_{4\gamma}\epsilon^*_\delta(\boldsymbol{k}_4,\lambda_4)\frac{-i}{t-m_a^2} \\ &\times\frac{i}{2}g\epsilon^{\mu\nu\rho\sigma}k_{1\mu}\epsilon_\nu(\boldsymbol{k}_1,\lambda_1)k_{3\rho}\epsilon^*_\sigma(\boldsymbol{k}_3,\lambda_3) \\ &+\frac{i}{2}g\epsilon^{\alpha\beta\gamma\delta}k_{2\alpha}\epsilon_\beta(\boldsymbol{k}_2,\lambda_2)k_{3\gamma}\epsilon^*_\delta(\boldsymbol{k}_3,\lambda_3)\frac{-i}{u-m_a^2} \\ &\times\frac{i}{2}g\epsilon^{\mu\nu\rho\sigma}k_{1\mu}\epsilon_\nu(\boldsymbol{k}_1,\lambda_1)k_{4\rho}\epsilon^*_\sigma(\boldsymbol{k}_4,\lambda_4). \end{aligned} \tag{49}$$

where $s=(k_1+k_2)^2=2k_1\cdot k_2$, $t=(k_1-k_3)^2=-2k_1\cdot k_3$ and $u=(k_1-k_4)^2=-2k_1\cdot k_4$.

We use the center-of-momentum frame, where $k_1=(\omega,\boldsymbol{k})$, $k_2=(\omega,-\boldsymbol{k})$, $k_3=(\omega',\boldsymbol{k}')$ and $k_4=(\omega',-\boldsymbol{k}')$. We have $s=2(\omega^2+\boldsymbol{k}^2)=4\omega^2$, $t=-2(\omega\omega'-\boldsymbol{k}\cdot\boldsymbol{k}')=-2\omega\omega'(1-\cos\theta)$ and $u=-2(\omega\omega'+\boldsymbol{k}\cdot\boldsymbol{k}')=-2\omega\omega'(1+\cos\theta)$, where θ is the scattering angle between $\boldsymbol{k}$ and $\boldsymbol{k}'$. Conservation of energy and momentum ensures that $s+t+u=0$, and implies that $\omega'=\omega$.

The differential cross section in the center-of-momentum frame for unpolarized photons is

$$\frac{d\sigma}{d\Omega}=\frac{1}{64\pi^2 s}\left(\frac{1}{4}\sum_{\lambda_1,\lambda_2,\lambda_3,\lambda_4}|\mathcal{M}|^2\right). \tag{50}$$

We consider scattering at angle $\theta=0$. Then the four-momenta $k_3=k_1$ and $k_4=k_2$, and the same polarization vectors are used to describe the corresponding initial and final photons that have the same momenta. In Cartesian coordinates, we may choose $k_1=k_3=(\omega,0,0,\omega)$ and linear polarization vectors $\epsilon(\boldsymbol{k}_1,1)=\epsilon(\boldsymbol{k}_3,1)=(0,1,0,0)$ and $\epsilon(\boldsymbol{k}_1,2)=\epsilon(\boldsymbol{k}_3,2)=(0,0,1,0)$. Correspondingly, we have $k_2=k_4=(\omega,0,0,-\omega)$ and polarization vectors $\epsilon(\boldsymbol{k}_2,1)=\epsilon(\boldsymbol{k}_4,1)=(0,1,0,0)$ and $\epsilon(\boldsymbol{k}_2,2)=\epsilon(\boldsymbol{k}_4,2)=(0,0,-1,0)$. Then we need to evaluate the vertices of the amplitude (49).

First consider the vertices in the s-channel contribution. In the vertices we have

$$\epsilon_{\mu\nu\rho\sigma}k_1^\mu\epsilon^\nu(\boldsymbol{k}_1,\lambda_1)k_2^\rho\epsilon^\sigma(\boldsymbol{k}_2,\lambda_2)=-2\omega^2J_{\lambda_1\lambda_2}, \tag{51}$$

and

$$\epsilon_{\mu\nu\rho\sigma}k_3^\mu\epsilon^{*\nu}(\boldsymbol{k}_3,\lambda_3)k_4^\rho\epsilon^{*\sigma}(\boldsymbol{k}_4,\lambda_4)=-2\omega^2J_{\lambda_3\lambda_4}, \tag{52}$$

where we introduced the two-dimensional anti-diagonal unit matrix $J=\begin{pmatrix}0&1\\1&0\end{pmatrix}$.

In the t-channel contribution, the two momenta involved in each vertex are identical, and consequently the contribution vanishes:

$$\begin{aligned} &\epsilon_{\mu\nu\rho\sigma}k_1^\mu\epsilon^\nu(\boldsymbol{k}_1,\lambda_1)k_3^\rho\epsilon^{*\sigma}(\boldsymbol{k}_3,\lambda_3) \\ &\quad=\epsilon_{\mu\nu\rho\sigma}k_1^\mu\epsilon^\nu(\boldsymbol{k}_1,\lambda_1)k_1^\rho\epsilon^{*\sigma}(\boldsymbol{k}_1,\lambda_3)=0, \end{aligned} \tag{53}$$

and

$$\begin{aligned} &\epsilon_{\mu\nu\rho\sigma}k_2^\mu\epsilon^\nu(\boldsymbol{k}_2,\lambda_2)k_4^\rho\epsilon^{*\sigma}(\boldsymbol{k}_4,\lambda_4) \\ &\quad=\epsilon_{\mu\nu\rho\sigma}k_2^\mu\epsilon^\nu(\boldsymbol{k}_2,\lambda_2)k_2^\rho\epsilon^{*\sigma}(\boldsymbol{k}_2,\lambda_4)=0. \end{aligned} \tag{54}$$

In the u-channel contribution, we obtain

$$\epsilon_{\mu\nu\rho\sigma}k_1^\mu\epsilon^\nu(\boldsymbol{k}_1,\lambda_1)k_4^\rho\epsilon^{*\sigma}(\boldsymbol{k}_4,\lambda_4)=-2\omega^2J_{\lambda_1\lambda_4}, \tag{55}$$

and

$$\epsilon_{\mu\nu\rho\sigma}k_2^\mu\epsilon^\nu(\boldsymbol{k}_2,\lambda_2)k_3^\rho\epsilon^{*\sigma}(\boldsymbol{k}_3,\lambda_3)=-2\omega^2J_{\lambda_2\lambda_3}. \tag{56}$$

The unpolarized squared amplitude for the scattering angle $\theta=0$ is

$$\begin{aligned} \frac{1}{4}\sum_{\lambda_1,\lambda_2,\lambda_3,\lambda_4}|\mathcal{M}(0)|^2 &= \frac{g^4\omega^8}{(s-m_a^2)^2} \\ &+\frac{g^4\omega^8}{2(s-m_a^2)(u-m_a^2)}+\frac{g^4\omega^8}{(u-m_a^2)^2}. \end{aligned} \tag{57}$$

For angle $\theta=0$ we have $s=u=4\omega^2$ and hence we obtain

$$\frac{1}{4}\sum_{\lambda_1,\lambda_2,\lambda_3,\lambda_4}|\mathcal{M}(0)|^2=\frac{5g^4\omega^8}{2(4\omega^2-m_a^2)^2}. \tag{58}$$

Thus the differential cross section (50) for unpolarized photons at the scattering angle $\theta=0$ is

$$\frac{d\sigma(0)}{d\Omega}=\frac{5g^4}{2^9\pi^2}\frac{\omega^6}{(4\omega^2-m_a^2)^2}. \tag{59}$$

3.2.2 Dispersion relation and the delay of gamma-rays

The contribution of axions to the photon plasma frequency is

$$\omega_p^2=\frac{\sqrt{5}Ng^2}{4\sqrt{2}}\sqrt{\frac{\omega^6}{(4\omega^2-m_a^2)^2}}=\frac{\sqrt{5}Ng^2}{16\sqrt{2}}\frac{\omega}{1-\frac{m_a^2}{4\omega^2}}, \tag{60}$$

where N is the number density of photons. In high energies $\omega\gg m_a^2$, we have

$$\omega_p^2=\frac{\sqrt{5}Ng^2}{16\sqrt{2}}\omega\left(1+\sum_{i=1}^{\infty}\left(\frac{m_a^2}{s}\right)^i\right)\simeq\frac{\sqrt{5}Ng^2}{16\sqrt{2}}\omega, \tag{61}$$

where $\omega=\sqrt{s}/2$ in terms of the invariant s.

The group velocity of gamma-rays in the photon medium is

$$v_{GRB}=1-d,\quad d=\frac{\sqrt{5}Ng^2}{32\sqrt{2}\omega}. \tag{62}$$

Using the photon number density of CMB, $N_\gamma=(4\text{–}5)\times10^8\ \mathrm{m}^{-3}$, and estimating the effective coupling constant to

be $g = 10^{-10}\,\mathrm{GeV}^{-1}$, the contribution of axion exchange to the GRB delay produced by CMB is given as

$$\tau_{\mathrm{CMB}} = \frac{3\times 10^{-54}}{\sqrt{\bar{E}}} \times \frac{D}{c}. \tag{63}$$

For GRB originating from the farthest galaxies ($D = 1.4\times 10^{26}$ m) the delay produced by the interaction with CMB is $\tau_{\mathrm{CMB}} = 2\times 10^{-36}\ \mathrm{s}/\sqrt{\bar{E}}$; e.g. for gamma-ray energy $E = 100$ GeV the delay is $\tau_{\mathrm{CMB}} = 2\times 10^{-37}$ s, which is a negligible delay.

4 Remarks on Lorentz invariance violation

The high energy tests of (an intrinsic) Lorentz invariance violation (LIV), as proposed by [43] with specific examples for them, have attracted considerable interest in connection with GRB; see e.g. [5–8,10,44–48]. We shall now compare the present light dispersion approach to the assumption of Lorentz invariance violation. Typically, in the LIV approach motivated by quantum gravity effects the dispersion relation contains higher-powers of energy,

$$E^2\left[1+\xi\frac{E}{E_{QG}}+O\left(\frac{E^2}{E_{QG}^2}\right)\right] = \boldsymbol{p}^2c^2+m^2c^4, \tag{64}$$

where E_{QG} is an effective energy scale for quantum gravity, commonly taken to be of order 10^{16} GeV, and ξ is an arbitrary parameter. The expression for the group velocity takes the following form to leading order in E/E_{QG},

$$v_g = c\left(1-\xi\frac{E}{E_{QG}}\right). \tag{65}$$

Then it is assumed that $\xi > 0$ so that v_g as the signal speed of radiation is subluminal. Thus, the higher energy of GRB, the greater slowdown of it.

Comparison with the dispersion relation (5) above leads to an interesting observation: the energy dependencies of the resulting GRB time delays are qualitatively different, which can be used to distinguish the two interpretations including their amounts experimentally. In the case of LIV, the time delay behaves as $\tau \propto E$. Dispersion in electron and axion media produces a time delay as $\tau \propto E^{-2}$. Thus, if gamma-rays with the highest energies arrive first, the conventional dispersive plasma theory with an electron-like coupling is supported, while if the highest-energy gamma-rays arrive later, the Lorentz invariance breaking dispersion relation is supported. It would be quite important to test out this issue experimentally. An observation of advance of the highest energy photons would imply that the LIV model would have to be reconsidered. In order to perform such a test, the spectrum of GRB needs to be recorded with as high temporal resolution as possible.

Since the LIV modification of the dispersion relation should effect particles of all kinds, and particularly both photons and neutrinos, it is difficult to explain the delays between GRB and neutrino bursts coming from the same source. In this interpretation such a delay could only be possible if the energy of neutrinos differs from the energy of photons by several orders of magnitude [7], which is hard to believe. However, if one would argue that in LIV the dispersions relations for photon and neutrino are different due to different quantum gravity effects on them, then by all means the whole effect should not be called LIV but the *induced* LIV.

It is noteworthy that it is not known experimentally whether the gamma-ray bursts arrive earlier, or later, than the neutrino bursts – the IceCube in Antarctica has detected some cosmic neutrinos, but they cannot be associated with any astrophysical object [49] (for a recent experiment at this detector, see [4]).

Finally, we would like to mention that an *intrinsic* violation of the Lorentz symmetry can be detected in several ways in precision experiments in different processes as has been in full details described in [43]. LIV can also occur in a way that differs from the hitherto used approach to LIV by changing the Special Relativity dispersion relation. For instance, the Lorentz group could be broken to certain proper subgroups of the Poincaré group, to the so-called Very Special Relativity [53]. It also can occur that the dispersion relation does not change but the Lorentz symmetry is broken – an example is the noncommutative field theory [50,51], where we have the residual twisted Poincaré symmetry [52].

5 Discussion and conclusions

We have considered the propagation of gamma-ray photons in the interstellar space – a problem of considerable interest by itself and analyzed in details the dispersion of light travelling through the interstellar space behaving as a plasma medium.

Dispersive properties of normal matter and background radiation, CMB, are insufficient to produce a significant GRB delay, when using some indicative densities of the constituent particles.

We have considered the media having nonrelativistic constituents – the nonrelativistic approximation can be justified since the main part of the GRB travel occurs in the interstellar space, where the delay actually occurs, and the temperature is so low (as in CMB) that the constituent particles of the media are practically frozen.

Then we have taken into account the effect of dark matter by assuming that dark matter consists of very light and cold particles, the hypothetical axions, with their theoretically expected coupling to photons. We find that for the hith-

erto realistic density of dark matter (revealed by its gravitational effect), the produced GRB delay is also very small.

The derived basic formulas for the time delay τ are given in Eq. (12) for an electron–positron plasma, in Eq. (14) for a photon plasma as CMB medium, in Eq. (47) for a Galactic Halo and in (48) for a massive galaxy filament. The numerical values in those equations are for the realistic values of the particle densities according to different estimates, or the ones considered to be more or less reasonable. The derivations of the light dispersion relation in all the different media in QFT are presented in the Appendix A and its subsections.

As seen from the Eqs. (12), (14), (47) and (48), the smallest delay for the high energy gamma-rays comes from dispersion in an axion plasma, and slightly larger delay for an electron–positron plasma.

The largest delay comes from the dispersion of light in a medium such as filled with CMB. In addition, the delay time as a function of the incoming photon energy in a medium filled with light radiation is $1/E^{3/2}$, while in an electron or axion medium it is $1/E^2$. Thus, at higher and higher energies the dispersion in light medium dominates over the other two media. The latter, is a quite important issue, since the value for the delay, which is proportional to the density of particles, given in Eq. (14) is estimated with the average density in CMB in only the observed part of the Universe, (being typically $\tau \sim 2 \times 10^{-8}$ s for a 100 GeV gamma-ray burst from farthest galaxies), while in other parts of the Universe the density of photons can be by far larger.

As already mentioned, we have considered the dispersion for each medium separately, in order to evaluate and find out which medium gives the largest delay for the dispersion of light, which comes out to be the CMB medium. Considering the total dispersion due to all the three media, gives simply the addition of each of them. This is easily seen from the derivation of dispersion relations in QFT and the fact that the interference terms among the scattering amplitudes with different final states do not give a contribution in the square of the absolute value of the sum in obtaining the cross section and thus the sum will be the addition of the absolute magnitudes of the diagrams with the same final states.

The very high energies and long travel distances of GRB have initiated to consider different models of Lorentz violation by modifying the (mass-energy-momentum) dispersion relations. Such an approach typically leads to a signal velocity as in Eq. (65), which decreases as a function of energy. We also see that such breaking of Special Relativity would lead to the simultaneous breaking of General Relativity, in which case many other results should be reconsidered and revalued. Thus, we believe that before invoking the drastic assumption of breaking of the Special Relativity to interpret GRB delays, one should also consider all possible ways to explain the phenomenon within the standard physics, a special case of which, namely the dispersion of light in the interstellar space, what always exists, has been presented in the present work.

As always, the decisive evidence will finally be given by experiment: in the case of the interpretation in terms of dispersion of light, the higher-energy gamma-rays arrive the Earth earlier and the lower-energy ones later, while in the typical LIV models hitherto presented based on quantum gravity effects such as in stringy foam models for the space, it occurs the opposite.

We should emphasize that all the models considered till now can only be called as an *induced* (seeming) LIV and not simply as LIV, which could imply *intrinsic* (genuine) LIV. The wording of simply LIV has been used for brevity in some recent literature instead of the *induced* LIV.

Concerning the experimental observation of an *intrinsic* (genuine) violation of the Lorentz invariance and its theoretical interpretation, we have already mentioned at the very end of Sect. 4 above, and referred to the seminal works in [43] and [53]. But we would like to recall that all the symmetries and laws derived from them are based on the existence of some group of symmetries, no matter whether they are global or local (gauge), internal or spacetime (external) symmetries and their breaking described by a residual or subgroup of the original groups of symmetries or an acceptable deformation of those groups, i.e. ones with their motivation not based on the presence of a medium such as gravity or curvature, but not breaking the Lorentz group in an arbitrary way. The same should be also in the case of the breaking of the Lorentz symmetry. The work in [53] is a good example, where the natural requirements for the residual group of symmetry, i.e. the broken ones, have been chosen to be a subgroup of the Poincaré group, and such that both the translational and CPT invariance remain preserved.

Several experiments, e.g. the recent Refs. [54–56], will analyze the energy-dependent delay in the arriving time of photons and will be able to resolve this issue. In the dispersive approach, the delay of an electromagnetic signal increases at lower photon energies. Therefore signals with radio frequencies would be a possible way to test the approach. Since the mass of axion is very low, possibly as low as $m_a \sim 10^{-18}$ eV, and our derivations hold for photons with energy much higher than the axion mass, our results may be applicable to many radio signals as well.

The observation of gravitational waves (GW) and a short GRB from the merger of two neutron stars in NGC 4993 [57,58] shows that gamma-ray photons do not experience long delays, since the GRB was observed only 1.7 seconds after the GW. Electromagnetic signals with lower frequencies were recorded by several teams starting eleven hours after the GW and ending weeks later, ranging from x-rays to radio frequencies [58]. Optical and infrared observations showed a towards-red evolution during 10 days. That is consistent with emissions from a cooling debris of the merger. We

remark two things. Firstly, the GRB delays caused by dispersion of gamma-rays in the cosmic medium, as derived in this work, are much shorter than the observed delay between GW 170817 and GRB 170817A signals, assuming that the GW are not effected by the medium. That is expected, since the gamma-rays are thought to be produced after the gravitational waves. Secondly, for the dispersive approach the dependency of the time delay on photon frequency (i.e. higher frequencies are delayed less than lower frequencies) is consistent with the observations of the merger. The same might not be the case with LIV models which exhibit an opposite relation between the time delay and the photon frequency.

In our estimates we have considered only the average axion densities at great distances, particularly at the level of galaxy filaments and in the dark matter halo of a typical galaxy. Any finer details of axion distribution have been neglected in these estimates. The same concerns the density of photons, such as in CMB, taken to be as in only the observed part of the Universe. Therefore, it would be enlightening to study the effects of different axion distributions, as well as the densities of the photons in the larger distances in greater detail. In this way, future studies of GRB delays produced by dispersion of light in media can also shed additional light on the microstructure of the Universe.

As some final remarks, we would like to emphasize the following points:

i) in the case of an *intrinsic* LIV, i.e. a *genuine* violation of the Special Relativity, when the usual dispersion relation between the energy, momentum and mass of a particle is changed, that means the Minkowski metric is changed. Consequently, the General Relativity, based on the generalisation of Minkowski metric/diffeomorphism invariance, will break too and its usual consequences cannot anymore be used for analysing the experimental data;

ii) in all the models so far proposed concerning the GRB with the arguments based on quantum gravity effects such as stringy foam, or connected to the curvature of the space and interpreting them as LIV, they are actually induced LIV. Although calling them LIV is intriguing, that is not correct;

iii) the dispersion relation being simply a kinematical equation, is *universal* and depends on the metric of the spacetime and not on the nature of a particle or on any moving body. Therefore, the above-mentioned kind of models for LIV cannot explain any delay of high energy GRB compared with neutrino bursts, since the tiny masses of neutrinos have no effect on the group velocity, unless one tries to invoke different interactions of the media with GRB and neutrino—per se they are *induced Lorentz invariance violations*.

Note added

After the completion of our work we were informed about two previous works [59] and [60] on the propagation of light in an axion or photon plasmas, respectively, in quite different aspects and using different methods of calculation but without addressing the issue of GRB delay.

The work in [59] gives a comprehensive account of dispersion of light in a relativistic plasma theory, including also some numerical evaluation of the results. Their model is somewhat different from ours, since it involves nonminimal gravitational interaction for the pseudoscalar (axion) field, and the axion field varying linearly with respect to time. A main objective of their work was to show that the phase velocity of transverse electromagnetic waves can also be less than c, providing the possibility of resonant plasma/waves interactions. Within the permitted space of parameters for the propagating electromagnetic waves, the squared plasma frequency, ω_p^2, and consequently the effective photon mass squared, m_γ^2, are positive (see Fig. 3).

The work [60] has considered the conversion of high-energy gamma-rays to axions and a dominant dispersion of light in a photon medium corresponding to CMB effect. Using the nonlinear Euler-Heisenberg electrodynamics Lagrangian they obtain a negative value for the squared effective photon mass, $m_\gamma^2 < 0$. That would correspond to a superluminal group velocity for GRB. We believe that this result is incorrect, possibly due to obscure way of calculating the plasma frequency ω_p^2 and obtaining a negative value for it. Using the same way of calculation for an axion medium, they would also obtain a negative value of ω_p^2.

Acknowledgements We are much grateful to Felix Aharonian, Stanley Deser, Merab Gogberashvili, Rodrigo Gracia-Ruiz, Friedrich Hehl, Archil Kobakhidze, Bo-Qiang Ma, Claus Montonen, Viatcheslav Mukhanov, Yuri Obukhov, Adam Schwimmer, Anca Tureanu and Grigory Volovik for many useful discussions at different stages of the work.

Data Availability Statement This manuscript has no associated data or the data will not be deposited. [Authors' comment: This research does not include data analysis.].

Funded by SCOAP[3].

Appendix A: Calculation of the plasma frequency from quantum field theory

Here we explain how the refraction index and the plasma frequency can be derived from quantum field theory. In order to

show how it works, we first consider the case of electrons and photons with standard quantum electrodynamics. Then we consider the axion with its interaction to the electromagnetic field (15). We use a system of units with Heaviside–Lorentz electromagnetic units and $\hbar = c = 1$.

Appendix A.1: Preliminaries on optical theorem

The refraction index is related to the forward scattering amplitude $f(0)$ (at zero scattering angle) as [61,62]

$$n = 1 + \frac{2\pi N f(0)}{\omega^2}, \tag{A.1}$$

where N is the number density of scatterers, that is the density of the constituents of the plasma. The relation (A.1) is valid when n is close to one, $|n-1| \ll 1$, and follows from the inteference between incident and scattered waves. In (A.1), n is a complex number, where the real part describes dispersion and the imaginary part describes absorption. Together with the relation $\mathrm{Im}\, n = 2\pi\, N\, \mathrm{Im}\, f(0)/\omega^2 = N\sigma/2\pi$ between the imaginary part of n and the absorption coefficient $N\sigma$, where σ is the total cross section, (A.1) leads to the Bohr–Peierls–Placzek relation [63] (see also [61,62]),

$$\sigma = \frac{4\pi\, \mathrm{Im}\, f(0)}{\omega}, \tag{A.2}$$

also known as the optical theorem.

We notice that within the perturbative quantum field theory the neglect of $\mathrm{Im}\, f(0)$ is naturally satisfied: one can see from (A.2) that the imaginary part of $f(0)$ is proportional to the cross section, which is proportional to the square of the amplitude and thus higher in the order of the small coupling constant than in the corresponding formula in (A.8), which is of the lower order in the coupling constant, being proportional to the amplitude itself.

Inserting (2) into (A.1) we obtain a relation between the plasma frequency and the scattering amplitude,

$$\sqrt{1 - \frac{\omega_p^2}{\omega^2}} = 1 + \frac{2\pi N\, \mathrm{Re}\, f(0)}{\omega^2}. \tag{A.3}$$

When the photon frequency is large compared to the plasma frequency, $\omega^2 \gg \omega_p^2$, we obtain

$$\omega_p^2 = -4\pi N\, \mathrm{Re}\, f(0). \tag{A.4}$$

The scattering amplitude $f(\theta)$ is defined as a part of the quantum mechanical wave function at large distance r from the scatterer,

$$\psi(\boldsymbol{r}) = C\left(e^{i\boldsymbol{k}\cdot\boldsymbol{r}} + f(\theta)\frac{e^{ikr}}{r}\right), \tag{A.5}$$

where C is a normalization factor. The differential cross section is given in terms of the scattering amplitude as

$$d\sigma(\theta) = |f(\theta)|^2 d\Omega. \tag{A.6}$$

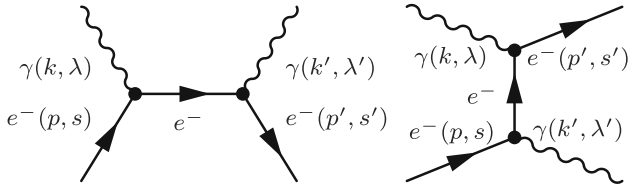

Fig. 3 Feynman diagrams for scattering of photon on electron

The closest thing to the scattering amplitude f in quantum field theory is the so-called T-matrix defined as the scattering part of the S-matrix

$$\langle\psi_f|S|\psi_i\rangle = \langle\psi_f|\psi_i\rangle + \langle\psi_f|iT|\psi_i\rangle. \tag{A.7}$$

The T-matrix, i.e. the Green's function, is related to the Feynman invariant scattering amplitude $\mathcal{M}$. In order to compute $f(0)$ in quantum field theory, we shall use the differential cross section. We calculate in quantum field theory the differential cross section $d\sigma(\theta)$ and from (A.6) the forward scattering amplitude follows as

$$|f(0)| = \left(\frac{d\sigma(0)}{d\Omega}\right)^{\frac{1}{2}}. \tag{A.8}$$

After the preliminaries presented above, we shall now proceed with the derivation of the plasma frequency for electron–positron plasma in standard quantum electrodynamics, as well as for a photon medium. Calculation of the plasma frequency for an electron–positron plasma is given here in order to show that our results coincide with the classical ones which have been derived before from the classical Maxwell equations.

Appendix A.2: Electron–positron plasma

Appendix A.2.1: Scattering amplitude in quantum electrodynamics

We consider photon–electron scattering $\gamma + e^- \to \gamma + e^-$ at tree level. The scattering amplitude $\mathcal{M}$ is a sum of the two diagrams in Fig. 3.

The incoming and outgoing electrons are represented by the Dirac spinors $u(\boldsymbol{p}, s)$ and $u(\boldsymbol{p}', s')$, respectively. The incoming and outgoing photons are represented by the polarization vectors $\epsilon_\mu(\boldsymbol{k}, \lambda)$ and $\epsilon_\mu^*(\boldsymbol{k}', \lambda')$, respectively. The amplitude in Feynman gauge is

$$\begin{aligned} i\mathcal{M} \;=\; & \bar{u}(\boldsymbol{p}', s')(-ie\gamma^\mu)\epsilon_\mu^*(\boldsymbol{k}', \lambda')\frac{i(\not{p} + \not{k} + m_e)}{(p+k)^2 - m_e^2} \\ & \times\epsilon_\nu(\boldsymbol{k}, \lambda)(-ie\gamma^\nu)u(\boldsymbol{p}, s) \\ & +\bar{u}(\boldsymbol{p}', s')(-ie\gamma^\nu)\epsilon_\nu(\boldsymbol{k}, \lambda)\frac{i(\not{p} - \not{k}' + m_e)}{(p-k')^2 - m_e^2} \\ & \times\epsilon_\mu^*(\boldsymbol{k}', \lambda')(-ie\gamma^\mu)u(\boldsymbol{p}, s) \end{aligned}$$

$$= -ie^2\epsilon^*_\mu(\boldsymbol{k}',\lambda')\epsilon_\nu(\boldsymbol{k},\lambda)\bar{u}(\boldsymbol{p}',s') \times\left(\frac{\gamma^\mu \not{k}\gamma^\nu + 2\gamma^\mu p^\nu}{2p\cdot k} + \frac{\gamma^\mu \not{k}'\gamma^\nu - 2\gamma^\nu p^\mu}{2p\cdot k'}\right)u(\boldsymbol{p},s), \tag{A.9}$$

where in the second equality we have written $p^2 = m_e^2$, $k^2 = 0$ and $(\not{p} + m_e)\gamma^\nu u(\boldsymbol{p},s) = 2p^\nu u(\boldsymbol{p},s)$.

The photons and electron are not polarized, and hence we average over initial spin states and sum over final spin states. In the squared Feynman amplitude, we use the spinor completeness relations and perform the resulting four traces of the γ-matrices. The result is

$$\frac{1}{4}\sum_{s,\lambda,s',\lambda'}|\mathcal{M}|^2 = 2e^4\left[\frac{p\cdot k'}{p\cdot k} + \frac{p\cdot k}{p\cdot k'} + 2m_e^2\left(\frac{1}{p\cdot k} - \frac{1}{p\cdot k'}\right) + m_e^4\left(\frac{1}{p\cdot k} - \frac{1}{p\cdot k'}\right)^2\right]. \tag{A.10}$$

In order to obtain the forward scattering amplitude $f(0)$, we obtain the differential cross section and compare to (A.8). The differential cross section is

$$d\sigma = \frac{1}{2k_0}\frac{1}{2p_0}\left(\frac{1}{4}\sum_{s,\lambda,s',\lambda'}|\mathcal{M}|^2\right)d\text{Lips}, \tag{A.11}$$

where the relative velocity of the initial particles is $c = 1$ (in any frame) and the Lorentz invariant two-body phase space is defined as

$$d\text{Lips} = (2\pi)^4\delta^4(k' + p' - k - p)\frac{d^3\boldsymbol{k}'}{(2\pi)^3 2k_0'}\frac{d^3\boldsymbol{p}'}{(2\pi)^3 2p_0'}. \tag{A.12}$$

Integration over $\boldsymbol{p}'$ is trivial and gives

$$d\text{Lips} = \frac{1}{(2\pi)^2 4k_0'p_0'}\delta(k_0 + p_0 - k_0' - p_0')d^3\boldsymbol{k}', \tag{A.13}$$

where $d^3\boldsymbol{k}' = \boldsymbol{k}'^2 d|\boldsymbol{k}'|d\Omega$. Since we consider a single scattering process in vacuum, the photon energy and momentum are related by the vacuum dispersion relation $k_0' = |\boldsymbol{k}'|$. Integration over $|\boldsymbol{k}'|$ gives

$$d\text{Lips} = \frac{(k_0 + p_0 - p_0')^2}{(2\pi)^2 4k_0'p_0'}d\Omega = \frac{k_0'}{(2\pi)^2 4p_0'}d\Omega. \tag{A.14}$$

We now choose the rest frame of the initial electron, $p = (m_e, \boldsymbol{0})$, and specialize to the case when the momenta of the initial and final photons are parallel. When $\boldsymbol{k}$ and $\boldsymbol{k}'$ are parallel, we have $k\cdot k' = k_0k_0' - \boldsymbol{k}\cdot\boldsymbol{k}' = |\boldsymbol{k}||\boldsymbol{k}'|(1-\cos\theta) = 0$, where $\theta = 0$ is the angle between $\boldsymbol{k}$ and $\boldsymbol{k}'$. We obtain from conservation of four-momentum that $(p + k - k')^2 = p'^2$, where the left-hand side is $m_e^2 + 2p\cdot k - 2p\cdot k' = m_e^2 + 2m_e(k_0 - k_0')$ and the right-hand side is m_e^2. This implies $k_0' = k_0$. Since energy is conserved, we also have $p_0' = p_0$. For $\theta = 0$ the squared Feynman amplitude (A.10) becomes

$$\frac{1}{4}\sum_{s,\lambda,s',\lambda'}|\mathcal{M}(0)|^2 = 4e^4. \tag{A.15}$$

Hence the differential cross section for $\theta = 0$ is

$$d\sigma(0) = \frac{1}{64\pi^2 m_e^2}\left(\frac{1}{4}\sum_{s,\lambda,s',\lambda'}|\mathcal{M}(0)|^2\right)d\Omega = \frac{e^4}{16\pi^2 m_e^2}d\Omega. \tag{A.16}$$

Comparing to (A.8) gives the absolute value of the forward scattering amplitude as

$$|f(0)| = \frac{\alpha}{m_e}, \tag{A.17}$$

where α is the fine-structure constant, $\alpha = \frac{e^2}{4\pi}$.

Appendix A.2.2: Electron–positron plasma frequency

The plasma frequency is obtained from (A.4) and (A.17) as

$$\omega_p^2 = \frac{4\pi\alpha N_e}{m_e} = \frac{N_e e^2}{m_e}. \tag{A.18}$$

This is the same result that is obtained from classical electrodynamics [18–20]. The electron–positron plasma frequency has also been obtained from quantum statistical physics by considering interaction in an electron–ion plasma [64].

5.1 Photon medium

The differential cross section of photon-photon scattering for high energy $\omega \gg m_e$ and the angle θ close to zero is given in the center-of-momentum frame as [33]

$$d\sigma = \frac{\alpha^4}{\pi^2\omega^2}\log^4\left(\frac{\omega}{m_e}\right)d\Omega, \quad \theta \ll \frac{m_e}{\omega}, \tag{A.19}$$

where $\omega = \sqrt{s}/2$.

The observations of GRB are performed in a frame where the GRB photons have very high energies, while the CMB photons have much lower energies. In such a frame, the average of s can be obtained by averaging over the angle between the momenta of the incoming photons for the scattering of GRB photons on CMB photons: $\langle s\rangle = \frac{1}{\pi}\int_0^\pi 2\omega_1\omega_2(1-\cos\phi)d\phi = 2\omega_1\omega_2$, where the GRB photon has energy ω_1, and the average energy of CMB photons can be obtained from blackbody radiation by dividing the energy density with photon number density: $\omega_2 = \frac{u(T)}{n(T)} = \frac{\frac{48\pi\zeta(4)}{c^3h^3}(k_BT)^4}{\frac{16\pi\zeta(3)}{c^3h^3}(k_BT)^3} = \frac{3\zeta(4)}{\zeta(3)}k_BT = 2.33\times10^{-4}\,\frac{\text{eV}}{\text{K}}\times T$. Hence we obtain a typical energy of the process as $\sqrt{\langle s\rangle} = \sqrt{\omega_1/\text{GeV}}\times 1.1$ keV.

References

1. E. Waxman, J.N. Bahcall, High-energy neutrinos from cosmological gamma-ray burst fireballs. Phys. Rev. Lett. **78**, 2292 (1997). https://doi.org/10.1103/PhysRevLett.78.2292. arXiv:astro-ph/9701231
2. M. Vietri, On the energy of neutrinos from gamma-ray bursts. Astrophys. J. **507**, 40 (1998). https://doi.org/10.1086/306336. arXiv:astro-ph/9806110
3. S. Adrián-Martínez et al., [ANTARES], Stacked search for time shifted high energy neutrinos from gamma ray bursts with the ANTARES neutrino telescope. Eur. Phys. J. C **77**, 20 (2017). https://doi.org/10.1140/epjc/s10052-016-4496-8. arXiv:1608.08840 [astro-ph.HE]
4. M.G. Aartsen et al., IceCube search for high-energy neutrino emission from TeV pulsar wind nebulae. Astrophys. J. **898**, 117 (2020). https://doi.org/10.3847/1538-4357/ab9fa0. arXiv:2003.12071 [astro-ph.HE]
5. G. Amelino-Camelia, J.R. Ellis, N.E. Mavromatos, D.V. Nanopoulos, S. Sarkar, Tests of quantum gravity from observations of gamma-ray bursts. Nature **393**, 763 (1998). https://doi.org/10.1038/31647. arXiv:astro-ph/9712103
6. J.R. Ellis, K. Farakos, N.E. Mavromatos, V.A. Mitsou, D.V. Nanopoulos, A search in gamma-ray burst data for nonconstancy of the velocity of light. Astrophys. J. **535**, 139 (2000). https://doi.org/10.1086/308825. arXiv:astro-ph/9907340
7. U. Jacob, T. Piran, Neutrinos from gamma-ray bursts as a tool to explore quantum-gravity-induced Lorentz violation. Nat. Phys. **3**, 87 (2007). https://doi.org/10.1038/nphys506. arXiv:hep-ph/0607145
8. U. Jacob, T. Piran, Lorentz-violation-induced arrival delays of cosmological particles. JCAP **0801**, 031 (2008). https://doi.org/10.1088/1475-7516/2008/01/031. arXiv:0712.2170 [astro-ph]
9. J.R. Ellis, N.E. Mavromatos, D.V. Nanopoulos, Derivation of a vacuum refractive index in a stringy space-time foam model. Phys. Lett. B **665**, 412 (2008). https://doi.org/10.1016/j.physletb.2008.06.029. arXiv:0804.3566 [hep-th]
10. G. Amelino-Camelia, J.R. Ellis, N.E. Mavromatos, D.V. Nanopoulos, Distance measurement and wave dispersion in a Liouville string approach to quantum gravity. Int. J. Mod. Phys A **12**, 607 (1997). https://doi.org/10.1142/S0217751X97000566. arXiv:hep-th/9605211
11. F. Wilczek, Two applications of axion electrodynamics. Phys. Rev. Lett. **58**, 1799 (1987). https://doi.org/10.1103/PhysRevLett.58.1799
12. G. Basar, G.V. Dunne, The chiral magnetic effect and axial anomalies. Lect. Notes Phys. **871**, 261 (2013). https://doi.org/10.1007/978-3-642-37305-3_10. arXiv:1207.4199 [hep-th]
13. A. Martín-Ruiz, M. Cambiaso, L.F. Urrutia, Green's function approach to Chern-Simons extended electrodynamics: an effective theory describing topological insulators. Phys. Rev. D **92**, 125015 (2015). https://doi.org/10.1103/PhysRevD.92.125015. arXiv:1511.01170 [cond-mat.other]
14. K. Fukushima, S. Imaki, Z. Qiu, Anomalous Casimir effect in axion electrodynamics. Phys. Rev. D **100**, 045013 (2019). https://doi.org/10.1103/PhysRevD.100.045013. arXiv:1906.08975 [hep-th]
15. P. Sikivie, Invisible axion search methods. Rev. Mod. Phys. **93**, 15004 (2021). https://doi.org/10.1103/RevModPhys.93.015004. arXiv:2003.02206 [hep-ph]
16. M. Gorghetto, E. Hardy, H. Nicolaescu, Observing invisible axions with gravitational waves. arXiv:2101.11007 [hep-ph]
17. N.E. Mavromatos, String quantum gravity, Lorentz-invariance violation and gamma-ray astronomy. Int. J. Mod. Phys. A **25**, 5409 (2010). https://doi.org/10.1142/S0217751X10050792. arXiv:1010.5354 [hep-th]
18. L. Tonks, I. Langmuir, Oscillations in ionized gases. Phys. Rev. **33**, 195 (1929). https://doi.org/10.1103/PhysRev.33.195
19. J.D. Jackson, *Classical Electrodynamics*, 3rd edn. (Wiley, New York, 1999)
20. M. Chaichian, I. Merches, D. Radu, A. Tureanu, *Electrodynamics: An Intensive Course* (Springer, Berlin, 2016)
21. P.W. Milonni, *Fast Light, Slow Light and Left-Handed Light* (Institute of Physics Publishing, 2005)
22. I.Y. Dodin, N.J. Fisch, On the evolution of linear waves in cosmological plasmas. Phys. Rev. D **82**, 044044 (2010). https://doi.org/10.1103/PhysRevD.82.044044
23. A. Fraser-McKelvie, K.A. Pimbblet, J.S. Lazendic, An estimate of the electron density in filaments of galaxies at $z \sim 0.1$. Mon. Not. R. Astron. Soc. **415**, 1961 (2011). https://doi.org/10.1111/j.1365-2966.2011.18847.x. arXiv:1104.0711 [astro-ph.CO]
24. D. d'Enterria, G.G. da Silveira, Observing light-by-light scattering at the Large Hadron Collider. Phys. Rev. Lett. **111**, 080405 (2013). https://doi.org/10.1103/PhysRevLett.111.080405. arXiv:1305.7142 [hep-ph]
25. A.M. Sirunyan et al., [CMS], Evidence for light-by-light scattering and searches for axion-like particles in ultraperipheral PbPb collisions at $\sqrt{s_{\mathrm{NN}}} = 5.02$ TeV. Phys. Lett. B **797**, 134826 (2019). https://doi.org/10.1016/j.physletb.2019.134826. arXiv:1810.04602 [hep-ex]
26. G. Aad et al., [ATLAS], Measurement of light-by-light scattering and search for axion-like particles with 2.2 nb^{-1} of Pb+Pb data with the ATLAS detector. arXiv:2008.05355 [hep-ex]
27. B. King, A. Di Piazza, C.H. Keitel, A matterless double slit. Nat. Photon. **4**, 92 (2010). https://doi.org/10.1038/nphoton.2009.261. arXiv:1301.7038 [physics.optics]
28. M. Marklund, Probing the quantum vacuum. Nat. Photon. **4**, 72 (2010). https://doi.org/10.1038/nphoton.2009.277
29. H. Euler, Über die Streuung von Licht an Licht nach der Diracschen Theorie. Ann. Phys. **26**, 398 (1936). https://doi.org/10.1002/andp.19364180503
30. W. Heisenberg, H. Euler, Folgerungen aus der Diracschen Theorie des Positrons. Z. Phys. **98**, 714 (1936). Consequences of Dirac Theory of the Positron. https://doi.org/10.1007/BF01343663. arXiv:physics/0605038
31. A. Akhiezer, Über die Streuung von Licht an Licht. Phys. Z. Sowjetunion **11**, 263 (1937)
32. R. Karplus, M. Neuman, The scattering of light by light. Phys. Rev. **83**, 776 (1951). https://doi.org/10.1103/PhysRev.83.776
33. V.B. Berestetskii, E.M. Lifshitz, L.P. Pitaevskii, *Quantum Electrodynamics* (Pergamon Press, Oxford, 1982)
34. S. Abdollahi et al., [Fermi-LAT Collaboration], A gamma-ray determination of the Universe's star formation history. Science **362**(6418), 1031 (2018). https://doi.org/10.1126/science.aat8123. arXiv:1812.01031 [astro-ph.HE]
35. E. Aliu et al., [MAGIC Collaboration], Very-high-energy gamma rays from a distant quasar: how transparent is the universe? Science **320**(5884), 1752 (2008). https://doi.org/10.1126/science.1157087. arXiv:0807.2822 [astro-ph]
36. F. Aharonian et al. [H.E.S.S.], A Low level of extragalactic background light as revealed by gamma-rays from blazars, Nature **440**, 1018 (2006). https://doi.org/10.1038/nature04680. arXiv:astro-ph/0508073
37. J. Halverson, C. Long, B. Nelson, G. Salinas, Towards string theory expectations for photon couplings to axionlike particles. Phys. Rev. D **100**, 106010 (2019). https://doi.org/10.1103/PhysRevD.100.106010. arXiv:1909.05257 [hep-th]
38. J.I. McDonald, L.B. Ventura, Optical properties of dynamical axion backgrounds. Phys. Rev. D **101**, 123503 (2020). https://doi.org/10.1103/PhysRevD.101.123503. arXiv:1911.10221 [hep-ph]
39. J.I. McDonald, L.B. Ventura, Bending of light in axion backgrounds. arXiv:2008.12923 [hep-ph]

40. T. Braine et al., [ADMX Collaboration], Extended search for the invisible axion with the axion dark matter experiment. Phys. Rev. Lett. **124**, 101303 (2020). https://doi.org/10.1103/PhysRevLett.124.101303. arXiv:1910.08638 [hep-ex]
41. Q.D. Jiang, F. Wilczek, Chiral Casimir forces: repulsive, enhanced, tunable. Phys. Rev. B **99**, 125403 (2019). https://doi.org/10.1103/PhysRevB.99.125403. arXiv:1805.07994 [cond-mat.mes-hall]
42. J.S. Høye, I. Brevik, Casimir force between ideal metal plates in a chiral vacuum. Eur. Phys. J. Plus **135**, 271 (2020). https://doi.org/10.1140/epjp/s13360-020-00267-1. arXiv:2002.01719 [quant-ph]
43. S.R. Coleman, S.L. Glashow, High-energy tests of Lorentz invariance. Phys. Rev. D **59**, 116008 (1999). https://doi.org/10.1103/PhysRevD.59.116008. arXiv:hep-ph/9812418
44. M. Rodriguez Martinez, T. Piran, Constraining Lorentz violations with gamma-ray bursts. JCAP **04**, 006 (2006). https://doi.org/10.1088/1475-7516/2006/04/006. arXiv:astro-ph/0601219
45. Z. Xiao, B.Q. Ma, Constraints on Lorentz invariance violation from gamma-ray burst GRB090510. Phys. Rev. D **80**, 116005 (2009). https://doi.org/10.1103/PhysRevD.80.116005. arXiv:0909.4927 [hep-ph]
46. L. Shao, Z. Xiao, B.Q. Ma, Lorentz violation from cosmological objects with very high energy photon emissions. Astropart. Phys. **33**, 312 (2010). https://doi.org/10.1016/j.astropartphys.2010.03.003. arXiv:0911.2276 [hep-ph]
47. S. Zhang, B.Q. Ma, Lorentz violation from gamma-ray bursts. Astropart. Phys. **61**, 108 (2015). https://doi.org/10.1016/j.astropartphys.2014.04.008. arXiv:1406.4568 [hep-ph]
48. C. Li, B.Q. Ma, Ultrahigh-energy photons from LHAASO as probes of Lorentz symmetry violations. arXiv:2105.07967 [astro-ph.HE]
49. R. Gracia-Ruiz, private communication
50. F. Ardalan, H. Arfaei, M.M. Sheikh-Jabbari, Noncommutative geometry from strings and branes. JHEP **9902**, 016 (1999). https://doi.org/10.1088/1126-6708/1999/02/016. arXiv:hep-th/9810072
51. N. Seiberg, E. Witten, String theory and noncommutative geometry. JHEP **9909**, 032 (1999). https://doi.org/10.1088/1126-6708/1999/09/032. arXiv:hep-th/9908142
52. M. Chaichian, P.P. Kulish, K. Nishijima, A. Tureanu, On a Lorentz-invariant interpretation of noncommutative space-time and its implications on noncommutative QFT. Phys. Lett. B **604**, 98 (2004). https://doi.org/10.1016/j.physletb.2004.10.045. arXiv:hep-th/0408069
53. A.G. Cohen, S.L. Glashow, Very special relativity. Phys. Rev. Lett. **97**, 021601 (2006). https://doi.org/10.1103/PhysRevLett.97.021601. arXiv:hep-ph/0601236 [hep-ph]
54. A. Albert et al., [HAWC Collaboration], Constraints on Lorentz invariance violation from HAWC observations of gamma rays above 100 TeV. Phys. Rev. Lett. **124**, 131101 (2020). https://doi.org/10.1103/PhysRevLett.124.131101. arXiv:1911.08070 [astro-ph.HE]
55. V.A. Acciari et al., [MAGIC], Observation of inverse Compton emission from a long γ-ray burst. Nature **575**, 459 (2019). https://doi.org/10.1038/s41586-019-1754-6. arXiv:2006.07251 [astro-ph.HE]
56. V.A. Acciari et al., [MAGIC Collaboration and Armenian Consortium: ICRANet-Armenia at NAS RA, A. Alikhanyan National Laboratory and Finnish MAGIC Consortium: Finnish Centre of Astronomy with ESO], Bounds on Lorentz invariance violation from MAGIC observation of GRB 190114C. Phys. Rev. Lett. **125**, 021301 (2020). https://doi.org/10.1103/PhysRevLett.125.021301. arXiv:2001.09728 [astro-ph.HE]
57. B.P. Abbott et al., [LIGO Scientific and Virgo Collaborations], GW170817: observation of gravitational waves from a binary neutron star inspiral. Phys. Rev. Lett. **119**, 161101 (2017). https://doi.org/10.1103/PhysRevLett.119.161101. arXiv:1710.05832 [gr-qc]
58. B.P. Abbott et al., [LIGO Scientific and Virgo and Fermi GBM and INTEGRAL and IceCube and IPN and Insight-Hxmt and ANTARES and Swift and Dark Energy Camera GW-EM and DES and DLT40 and GRAWITA and Fermi-LAT and ATCA and ASKAP and OzGrav and DWF (Deeper Wider Faster Program) and AST3 and CAASTRO and VINROUGE and MASTER and J-GEM and GROWTH and JAGWAR and CaltechNRAO and TTU-NRAO and NuSTAR and Pan-STARRS and KU and Nordic Optical Telescope and ePESSTO and GROND and Texas Tech University and TOROS and BOOTES and MWA and CALET and IKI-GW Follow-up and H.E.S.S. and LOFAR and LWA and HAWC and Pierre Auger and ALMA and Pi of Sky and DFN and ATLAS Telescopes and High Time Resolution Universe Survey and RIMAS and RATIR and SKA South Africa/MeerKAT Collaborations and AstroSat Cadmium Zinc Telluride Imager Team and AGILE Team and 1M2H Team and Las Cumbres Observatory Group and MAXI Team and TZAC Consortium and SALT Group and Euro VLBI Team and Chandra Team at McGill University], Multi-messenger Observations of a Binary Neutron Star Merger. Astrophys. J. Lett. **848**, L12 (2017). https://doi.org/10.3847/2041-8213/aa91c9. arXiv:1710.05833 [astro-ph.HE]
59. A.B. Balakin, R.K. Muharlyamov, A.E. Zayats, Electromagnetic waves in an axion-active relativistic plasma non-minimally coupled to gravity. Eur. Phys. J. C **73**, 2647 (2013). https://doi.org/10.1140/epjc/s10052-013-2647-8. arXiv:1310.5333 [gr-qc]
60. A. Dobrynina, A. Kartavtsev, G. Raffelt, Photon-photon dispersion of TeV gamma rays and its role for photon-ALP conversion. Phys. Rev. D **91**, 083003 (2015). https://doi.org/10.1103/PhysRevD.91.083003. arXiv:1412.4777 [astro-ph.HE]
61. J.M. Jauch, F. Rohrlich, *The Theory of Photons and Electrons: The Relativistic Quantum Field Theory of Charged Particles with Spin One-Half*, 2nd edn. (Springer, Berlin, 1976)
62. R.G. Newton, *Scattering Theory of Waves and Particles*, 2nd edn. (Springer, Berlin, 1982)
63. N. Bohr, R. Peierls, G. Placzek, Nuclear reactions in the continuous energy region. Nature **144**, 200 (1939). https://doi.org/10.1038/144200a0
64. A.A. Abrikosov, L.P. Gorkov, I.E. Dzyaloshinski, *Methods of Quantum Field Theory in Statistical Physics* (Prentice-Hall, Englewood Cliffs, 1963)